

Short-range correlations and the nuclear momentum density distribution for ¹⁶O

J. W. Van Orden, W. Truex, and M. K. Banerjee

Department of Physics and Astronomy, University of Maryland, College Park, Maryland 20742

(Received 19 November 1979)

The leading-order correlation corrections to the independent particle shell model momentum density distribution for ¹⁶O are calculated using the Brueckner theory of finite nuclei. The Pauli corrected defect functions are calculated using Reid soft core B and de Tourreil-Sprung interaction potentials with harmonic oscillator starting wave functions and experimental shell model starting energies. The short-range correlations are found to modify significantly the independent particle shell model momentum density distribution for low momenta and to dominate it for high momenta. Comments are made concerning the selection of ground state nuclear wave functions for calculating quasielastic scattering processes.

[NUCLEAR STRUCTURE ¹⁶O, calculated momentum density distribution.]
 [Brueckner method finite nuclei; Reid soft core, Sprang potentials used.]

The experiments of Frankel *et al.*¹ with 180° proton production from quasielastic proton-nucleus scattering have stimulated interest in the nuclear momentum density distribution. A simplified calculation of this process which is roughly dependent upon the nuclear momentum distribution has been used in an attempt to extract this distribution from the data.²

As a result of this interest in the momentum distribution, Zabolitzky and Ey³ have produced theoretical calculations of the momentum density distribution using the coupled-cluster or exp(S) form of many-body theory⁴ in the generalized Brueckner-Hartree-Fock approximation. The calculations in Ref. 3 show that the momentum distribution is dominated by two-nucleon correlation contributions at momenta greater than 2 fm⁻¹. This suggests the value of an experimental determination of the nuclear momentum distribution as a possible means of studying two-body correlations. Therefore, it is necessary to perform more realistic calculations of 180° proton production or similar processes such as quasielastic electron scattering in order to determine whether it is possible to obtain the nuclear momentum distribution, or comparable information concerning nuclear correlations, from such experiments.

With this eventual object in mind, we will present first the simpler approach of the Brueckner theory of finite nuclei⁵ to introduce two-nucleon correlations. This approach will be used to calculate the momentum density distributions for ¹⁶O using Reid soft core B and de Tourreil-Sprung potentials. These will be shown to be essentially equivalent to those of Ref. 3. We will then make use of the momentum distributions to discuss whether it is necessary to use more realistic single-nucleon ground state wave functions such as

those due to a Woods-Saxon potential.

We define the momentum density distribution $n(p)$ with the following normalization:

$$A = \frac{1}{(2\pi)^3} \int d^3p n(p), \tag{1}$$

where A is the total number of nucleons.

Using the Brueckner theory for finite nuclei, the nuclear momentum density distribution including the lowest-order two-nucleon correlation corrections is represented by the Goldstone diagrams of Figs. 1(a)-(e), where the cross repre-

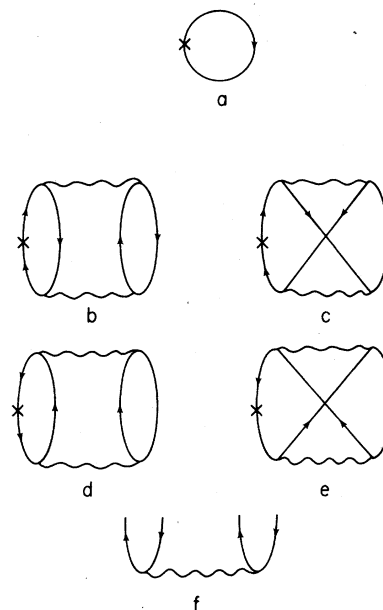


FIG. 1. Goldstone diagrams representing momentum density distribution with lowest order two-nucleon correlation corrections.

sents the nonlocal operator $e^{i\vec{p}\cdot(\vec{r}'-\vec{r})}$, the wavy lines represent the two-nucleon interaction resulting from the sum of ladder diagrams, and the upward and downward pointing arrows represent particles and holes, respectively.

Diagram 1(a) represents the independent particle shell-model result for the momentum distribution while diagrams 1(b)–1(e) represent the lowest-order two-nucleon correlation corrections to the momentum density. Diagrams 1(d) and 1(e) serve to renormalize diagram 1(a) such that the total number of nucleons remains unchanged by the introduction of correlations. The actual calculation of these diagrams can be simplified by recognizing that the parts of each of the diagrams 1(b)–1(e) corresponding to Fig. 1(f) represent the two-nucleon defect function which is defined as the difference between the Brueckner-Hartree-Fock (BHF) pair wave function and the exact, correlated pair wave function. The defect function can be determined from the equation

$$|\chi\rangle = |\phi\rangle - |\psi\rangle = -\frac{Q}{\omega - H_0} V |\psi\rangle, \quad (2)$$

where $|\psi\rangle$ and $|\phi\rangle$ are the exact and BHF two-nucleon wave functions, V is the interaction potential, H_0 is the BHF Hamiltonian, ω is the energy of the two-nucleon propagator, and Q is the Pauli operator.

The evaluation of Eq. (2) is simplified in this work by introducing several approximations. The most important of these is the replacement of the BHF wave functions by harmonic oscillator ground state wave functions where the oscillator parameter is chosen to provide a good fit to the low momentum (≤ 400 MeV) portion of the elastic charge form factor. This eliminates the problem of actually finding solutions to the self-consistent BHF equations. Such solutions do not always give accurate binding energies and do not always provide a good description of the elastic charge form factor.^{3,4,6} A more practical consideration is the obvious convenience of having an analytical expression for these wave functions and of being able to separate exactly pair wave functions into relative and center-of-mass factors by means of Moshinsky brackets. The additional approximations are made that the experimental shell-model binding energies are substituted for the eigenvalues of H_0 in Eq. (2), and that the Pauli operator Q is treated in the Eden-Emery approximation.

Using the above approximations, Eq. (2) is solved in coordinate space for both the Reid soft core B and de Tourreil-Sprung supersoft core potentials. The momentum distribution for ^{16}O is cal-

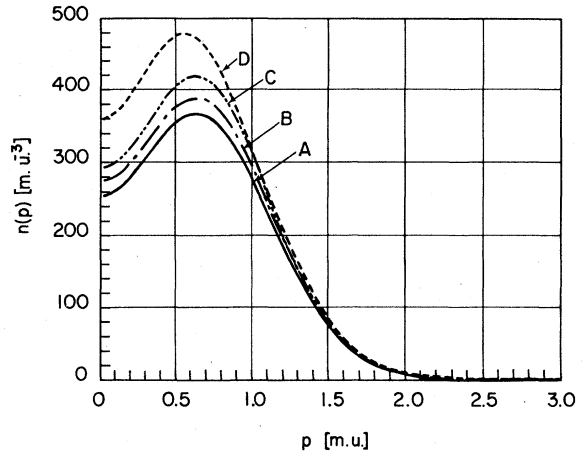


FIG. 2. Momentum density distribution for ^{16}O : 1 m.u. = $m_p c = 139.57$ MeV.

culated using the momentum space Fourier transform of the defect function corresponding to each potential. The accuracy of these calculations is tested by computing the norm of the defect functions calculated in both coordinate and momentum spaces, and by verifying that Eq. (1) is satisfied for each distribution. The resulting momentum distributions for ^{16}O are shown in Figs. 2 and 3 where line A represents the correlated distribution using the Reid potential, and line B is the correlated distribution using the Sprung potential. Line C is the IPSM harmonic oscillator momentum distribution and line D is the IPSM Woods-Saxon momentum distribution. Distributions A, B, and C have been corrected for spurious center-of-mass motion as in Ref. 3. Calculation of such a correction for the Woods-Saxon distribution is considerably more complicated

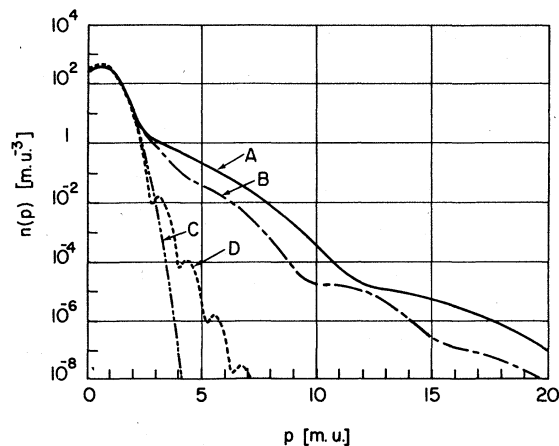


FIG. 3. Momentum density distribution for ^{16}O .

than for the distributions *A* through *C*, and is beyond the scope of this paper. For this reason the Woods-Saxon distribution (*D*) does not include corrections for spurious center-of-mass motion and is included only for the purpose of comparison with *C*. The momentum distributions displayed in Figs. 2 and 3 are in good agreement with the corresponding distributions in Ref. 3.

At low momenta the primary effect of the correlation is the renormalization of the IPSM distribution (*C*). At a momentum of approximately 2 mesic units (m.u., 1 m.u. = $m_p c = 139.57$ MeV) the correlated distributions (*A* and *B*) become larger than the uncorrelated distribution (*C*). At a momentum of 3 mesic units the correlated distributions are almost an order of magnitude larger than the uncorrelated distribution. At small momenta the Sprung distribution (*B*) is larger than the Reid distribution (*A*) and is smaller than the Reid distribution at large momenta, as would be expected.

It is interesting to consider the IPSM Woods-Saxon distribution (*D*). This distribution is larger at low momenta (less than 1 m.u.) than the harmonic oscillator distribution (*C*) since the Woods-Saxon potential is broader than the harmonic oscillator potential. As the momentum increases above 1 m.u. the harmonic oscillator distribution becomes larger than the Woods-Saxon distribution. At approximately 3 m.u. the Woods-Saxon distribution begins to show the oscillatory behavior which reflects the range parameter of the Woods-Saxon potential,⁷ and again becomes larger than the harmonic oscillator distribution at approximately 4 m.u. Examination of Fig. 3 shows the essentially exponential falloff of the Woods-Saxon density as opposed to the much more rapid Gaussian falloff of the harmonic oscillator density. The high momentum behavior of the Woods-Saxon wave functions is often considered to be more realistic than that of the harmonic oscillator wave function. However, at momenta above 2 m.u. the Woods-Saxon density (*D*) is much smaller than the correlated densities (*A* and *B*). The slower falloff and extra structure of the Woods-Saxon wave functions at large momenta is totally obscured by the two-nucleon correlations. Therefore, for processes which are roughly dependent upon the ground state momentum distribution, such as quasielastic proton or electron scattering, the ground state may be well described by harmonic oscillator wave functions and two-nucleon correlations.

The effect of correlations is quite different in the case of the elastic charge form factor than in the case of the momentum distribution. Figure 4 shows the elastic charge form factor for ¹⁶O

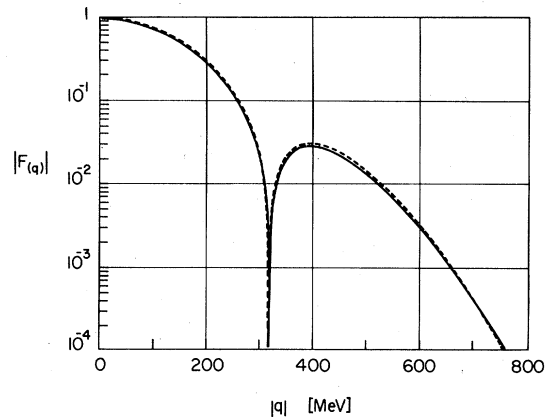


FIG. 4. Elastic charge form factor for ¹⁶O.

as calculated using the harmonic oscillator wave functions with (solid line) and without (dashed line) correlations. The correlations are included by evaluating a set of diagrams similar to Figs. 1(a)–1(e) where the cross represents the local operator $e^{i\vec{q}\cdot\vec{r}}$. Clearly in this case the inclusion of two-nucleon correlations results in negligible change to the elastic charge form factor. This tends to justify our use of the form factor as a means of selecting the oscillator parameter. Zabolitzky and Ey³ argue that the form factor is relatively insensitive to correlations since it is a measure of density fluctuations whereas the momentum density distribution is a measure of density correlations and is therefore much more sensitive to the inclusion of correlations.

In summary, we make the following conclusions:

(1) The simplified approach of Brueckner theory used in this paper provides a good description of the nuclear momentum density distributions. These distributions are in good agreement with those calculated in Ref. 3, using the much more complicated $\exp(S)$ method.

(2) At momenta less than 3 mesic units the renormalized single-particle momentum distribution dominates, whereas at momenta greater than 3 mesic units the correlation contributions to the momentum distribution dominate.

(3) Since correlation contributions dominate the momentum distribution at momenta greater than 3 mesic units, the high momentum behavior of the Woods-Saxon distribution is totally obscured by the correlations. Therefore, for processes which are roughly dependent upon the ground state momentum distribution, such as quasielastic proton or electron scattering, the ground state may be well described by harmonic oscillator wave functions and two-nucleon correlations.

(4) Since the elastic charge form factor is in-

sensitive to correlations, single-particle ground state wave functions may be selected by fitting the lower momentum ($|q| \lesssim 400$ MeV) portion of the elastic charge form factor.

The authors wish to acknowledge the support of the U. S. Department of Energy and the University of Maryland Computer Science Center for this work.

¹S. Frankel *et al.*, Phys. Rev. Lett. 36, 642 (1976).

²R. D. Amado and R. M. Woloshyn, Phys. Rev. Lett. 36, 1435 (1976).

³J. G. Zabolitzky and W. Ey, Phys. Lett. 76B, 527 (1978).

⁴J. G. Zabolitzky, Nucl. Phys. A228, 272 (1974).

⁵M. Baranger, *Proceedings of the International School of Physics "Enrico Fermi," Vol. 40*, Varena, Italy (Academic, New York, 1969), p. 511.

⁶M. Gari, H. Hyuga, and J. G. Zabolitzky, Nucl. Phys. A271, 365 (1976).

⁷The oscillatory behavior of line *D* in Fig. 3 reflects the well radius of the Woods-Saxon potential. The oscillations have a periodicity of $2\pi/(\text{well radius})$. A well radius of 2.68 m.u. was used in the calculation displayed in Figs. 2 and 3.